

DEVELOPMENT OF AN EXTREME ENVIRONMENT DC MOTOR DRIVE FULL BRIDGE POWER STAGE USING COMMERCIAL-OFF-THE-SHELF COMPONENTS

John Garrett⁽¹⁾, Roberto Schupbach⁽¹⁾, H. Alan Mantooth⁽²⁾, Alexander B. Lostetter⁽¹⁾

⁽¹⁾Arkansas Power Electronics International, Inc., 700 Research Center Blvd., Fayetteville, AR 72701, USA,
Email: john@apei.net

⁽²⁾University of Arkansas, Fayetteville, AR 72701, USA, Email: mantooth@uark.edu

Abstract – Spacecraft electronic systems routinely experience extreme environmental conditions, including cryogenic temperatures. Radioisotope Heating Units (RHUs) are commonly used to keep the electronic systems at warmer temperatures; however, the RHUs continually produce heat, are expensive, and add complexity and weight to the spacecraft. Previous research efforts have shown several commercial-off-the-shelf (COTS) components, both active and passive, can perform well in cryogenic environments, thus allowing for lower weight and complexity of the electronic systems aboard spacecraft. This paper details the cryogenic testing (down to -184 °C) of COTS components commonly used in DC motor drive power stages. The performance of silicon carbide (SiC) diodes and transistors at cold temperatures was evaluated, followed by the building and testing (down to -184 °C) of a cryogenic 20 W full bridge power stage for motor drive applications.

1. INTRODUCTION

Spacecraft electronic systems which experience cryogenic temperatures in their mission lifetimes are normally heated to more suitable temperatures for operation (i.e. 20 °C). This is done through the use of Radioisotope Heating Units (RHUs). Since RHUs constantly produce heat, thermal systems must be installed on the spacecraft to dissipate the heat when it is not needed, adding complexity and weight to the vehicle that could be better utilized. RHUs could potentially be eliminated through the use of commercial-off-the-shelf (COTS) components that have been found to operate reliably in these extreme environments. The COTS components studied in this research included the following elements that are commonly used in motor drives: resistors, capacitors, gate driver integrated circuits, diodes, and transistors. For each component, several technologies were evaluated in order to determine which technology could potentially yield the best performance at cold temperatures. Emerging silicon carbide (SiC) device technology was evaluated as well.

This paper is divided into seven sections. The second section discusses the overall test setup and the procedures followed for the cryogenic testing. The results of the cryogenic testing of the COTS components, component specific tests, as well as the additional equipment utilized to conduct the tests are presented in sections three and four. Section three details the passive elements tests and results, while section four details the active elements tests and results. The COTS components selection and the construction of the DC motor drive power stage are detailed in section five, followed by conclusions and references in sections six and seven, respectively.

2. TEST SETUP AND PROCEDURES

The cryogenic testing of the components and the power stage was conducted using a Delta Design 9028 environmental test chamber configured to use liquid nitrogen as a coolant to achieve the various cold temperatures down to -184 °C. The components were placed inside the chamber and the tests were performed at different temperatures. The resistors, capacitors, high/low side gate drivers, and power stage were each tested at the following temperatures in the specified sequence: +25 °C, 0 °C, -55 °C, -100 °C, -125 °C, -150 °C, -175 °C, and -184 °C. The diodes and transistors were tested at the following temperatures in the specified sequence: +25 °C, 0 °C, -55 °C, -100 °C, -150 °C, and -184 °C.

Each component was allowed to soak at each temperature for 15 minutes to ensure that its internal temperature reached steady state before any test circuits were energized to investigate the component's performance. After cryogenic testing, each component was allowed to warm to room temperature (+25 °C) and then retested to see what effects a single temperature cycle might have had on its performance.

3. PASSIVE ELEMENTS

3.1 Resistors

Resistors are a crucial part in gate drive and dead-time setting circuits. Nine resistor types were cryogenically tested in order to determine the performance of the different technologies at cryogenic temperatures, including; thick film, thin film, metal film, metal oxide, vitreous enamel, and metal foil resistors. The resistance of each resistor was measured with an HP 4261A LCR meter. Fig. 1 shows the results of the resistor tests versus temperature. In this figure, the resistances indicated are normalized to each individual resistor's room temperature resistance. It can be seen that most of the resistors demonstrated good performance over temperature, while a few did not. Most notably, the Ohmite thick film and the metal oxide resistors performed relatively poorly. When the resistors were retested at room temperature, it was observed that the single temperature cycle had little effect on most of the resistors. Two of the resistor types (Ohmite thick film and metal oxide) suffered some increases in resistance (0.01% and 0.36%, respectively) after the temperature cycle. From the results it can be seen that most of the resistors would be good for cryogenic applications except for the Ohmite thick film and the metal oxide resistors.

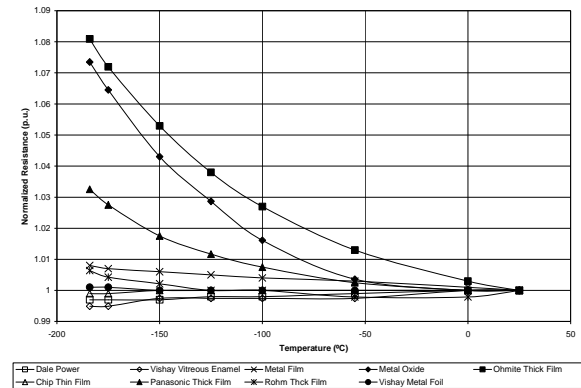


Fig. 1. Normalized resistance (p.u.) vs. temperature.

3.2 Capacitors

High performance capacitors are vital in most motor drive circuits. They are used for filtering and for providing instantaneous power to circuits under quick load changes.

Eight different types of capacitors were cryogenically tested in order to evaluate the performance of several capacitor technologies. These included the following: metallized polypropylene, polypropylene, polyethylene, NPO, X7R, and several tantalums. Both the capacitance and dissipation factor of each capacitor was

tested with and without a 30 VDC bias placed across the capacitor using a HP 4261A LCR meter and an external voltage source. The LCR meter was operated with the test frequency selector set for 1 kHz.

Fig. 2 and Fig. 3 show the results of the capacitor tests versus temperature where each capacitor has a 30 VDC bias placed across it. In Fig. 2, the capacitances indicated are normalized to each individual capacitor's room temperature capacitance. It is observed that the NPO, metallized polypropylene, and polypropylene types of capacitors exhibited slight increases in capacitance as their temperature was lowered. The remainder of the capacitors exhibited a decrease in capacitance as the temperature was lowered. Notably, the polyethylene and all of the tantalum types showed a decrease of less than 10% of their room temperature capacitance, whereas the X7R type showed the worst performance, a capacitance at -184 °C that was approximately 41% of its room temperature capacitance. In Fig. 3, the dissipation factor of each capacitor is shown. From the figure it can be seen that all three tantalum capacitors and the X7R performed relatively poorly compared to the other capacitors.

When the capacitors were retested at room temperature, it was observed that all but one was affected in terms of capacitance after a single temperature cycle. The X7R type suffered a 5.36% decrease in capacitance with no DC bias placed across it, and a 0.94% decrease in capacitance with a 30 VDC bias placed across it. There was no change observed in the dissipation factors.

From the results, it can be concluded that the metallized polypropylene, polypropylene, polyethylene, and NPO types would be the best choice for cold temperature applications. Tantalum types would also be good choices if the application requires higher energy storage capabilities, provided that the larger dissipation factors are acceptable.

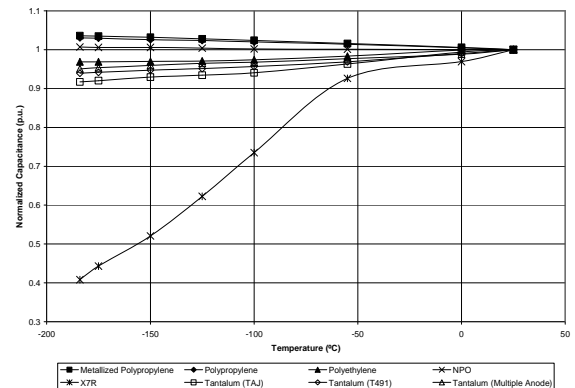


Fig. 2. Normalized capacitance (p.u.) vs. temperature.

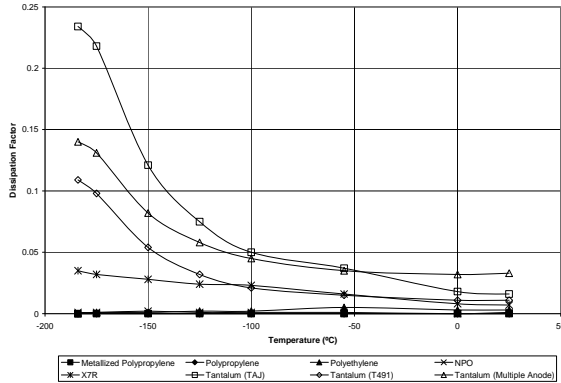


Fig. 3. Dissipation factor vs. temperature.

4. ACTIVE ELEMENTS

4.1 High/Low Side Gate Drivers

It is often necessary to use high/low side gate drivers in order to properly charge and discharge the large capacitances of power switching devices effectively, to provide isolation, and/or to generate a high side signal to drive the high side device in a half bridge.

Two different gate driver integrated circuit technologies were evaluated; silicon and silicon-on-insulator (SOI). Gate drivers based on BJT technology were not examined in this work due to recent research efforts indicating relatively poor performances of bipolar based integrated circuits at cold temperature [2,3]. Three gate drivers fabricated with silicon processes and one gate driver fabricated with an SOI process were chosen to be examined. The three silicon devices were the following: an IR2110S from International Rectifier, a L6385 from ST Microelectronics, and a MIC4100YM from Micrel Incorporated. The SOI gate driver chosen was the Phillips UBA2033. It is a high frequency full bridge driver IC designed as a commutator for high intensity discharge lamps, but can be configured to be a half bridge driver.

The performance of the gate drivers was evaluated by measuring the following time durations of the low side output while driving an external 1000pF capacitive load: turn-on propagation delay, turn-off propagation delay, turn-on rise time, and turn-off fall time. In addition, the supply current drawn by each gate driver was measured as the temperature was decreased. The measurement method used for the time duration measurements can be more clearly understood by referencing Fig. 4

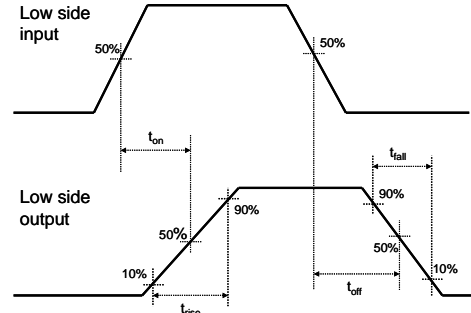


Fig. 4. Description of high/low side driver measurements.

A 20 kHz, 50% duty cycle square wave signal with an amplitude of 10 Volts was applied to the input of the drivers if independent low and high side inputs were available on the driver. If the driver did not have independent inputs, the same square wave signal would be applied to the single input available. A 15 VDC supply voltage was applied to the three silicon drivers, whereas a 13 VDC supply voltage was applied to the Phillips SOI driver. The input supply current was measured with a Tektronix DM 502A multi-meter. The cursor functionality of a Tektronix TDS 3014B oscilloscope was used to measure the turn-on rise time, turn-off fall time, turn-on propagation delay, and turn-off propagation delay of the low side output of each driver.

Fig. 5 through Fig. 8 show the turn-on propagation delay, turn-off propagation delay, turn-on rise time, and turn-off fall time of the gate drivers. From the results, it was seen that the Micrel MIC4100YM provided the best performance in terms of the change (smallest) in the time durations measured as the temperature was decreased. On the other hand, the SOI-based gate driver exhibited the largest change in the measured time durations as the temperature was decreased.

Fig. 9 shows the current supplied to each gate driver versus temperature. The IR2110S and the MIC4100YM both exhibited an increase in supply current as the temperature was decreased, whereas the ST L6385 showed a decrease in supply current as the temperature was decreased. The SOI driver exhibited both a rise and then a fall in the supply current as the temperature was decreased.

When the gate drivers were retested at room temperature, it was observed that the single temperature cycle had no effect on the gate drivers examined. From the test results, it can be seen that the silicon gate drivers provided the best performance when compared to the SOI gate driver at cryogenic temperatures. The Micrel MIC4100YM provided the best performance overall.

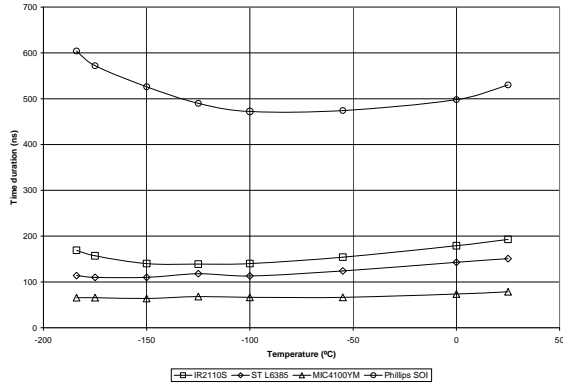


Fig. 5. Driver turn-on propagation delay vs. temperature.

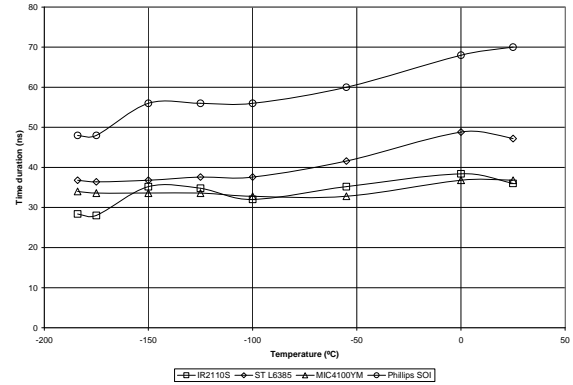


Fig. 8. Driver turn-off fall time vs. temperature.

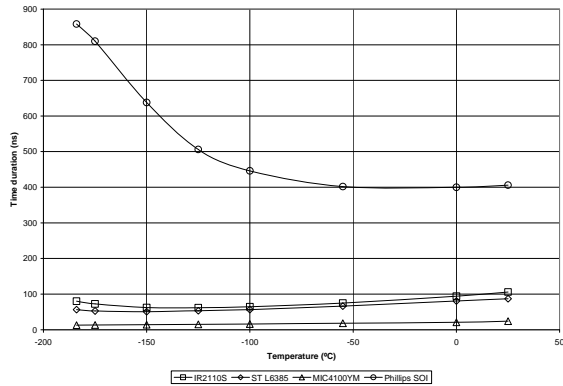


Fig. 6. Driver turn-off propagation delay vs. temperature.

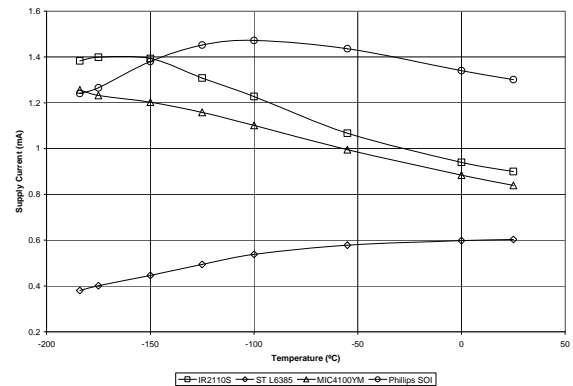


Fig. 9. Driver supply current vs. temperature.

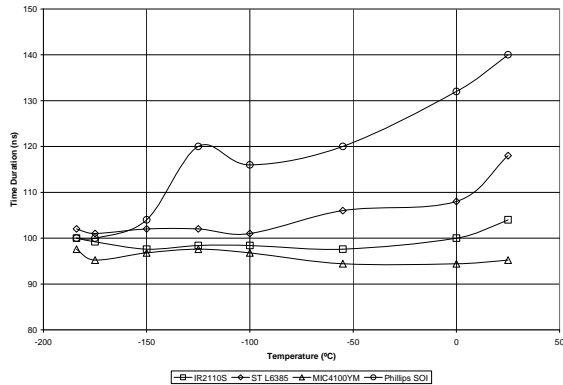


Fig. 7. Driver turn-on rise time vs. temperature.

4.2 Diodes and Transistors

Diodes and transistors that perform well at cryogenic temperatures are essential in order to efficiently and properly control the flow of power in power electronic circuits. For the diodes, three different technologies were evaluated: silicon schottky, silicon super-fast, and SiC schottky.

The following diodes were chosen to be tested: a 3 Amp 60 Volt silicon MBRS360TR schottky rectifier from International Rectifier, a 2 Amp 50 Volt silicon ES2A super-fast rectifier from Diodes Incorporated, and a 10 Amp 300 Volt SiC CSD10030 schottky diode from Cree. A Tektronix 371B programmable high power curve tracer was utilized to measure the forward voltages, on-resistances, and reverse breakdown voltages.

Fig. 10 through Fig. 12 show the diode forward voltages, on-resistances, and reverse breakdown voltages versus temperature. The results indicated that the silicon diodes followed roughly linear trends as the temperature decreased. On the other hand, the SiC diode did not follow this trend. In Fig. 10, it can be

observed that the forward voltage for each of the silicon diodes increased in a linear fashion as the temperature was lowered, whereas the forward voltage for the SiC diode increased in a non-linear manner. The on-resistances of the diodes, as seen in Fig. 11, show a similar behavior. Here, as the temperature is decreased, the on-resistances of the silicon diodes decrease almost linearly; however, the on-resistance of the SiC diode increases dramatically. In Fig. 12 the reverse breakdown voltages changed very little with respect to decreasing temperature. The silicon super-fast diode reverse breakdown voltage stayed approximately the same. The silicon schottky diode reverse breakdown voltage decreased slightly, whereas the breakdown voltage of the SiC schottky showed a small increase.

When the diodes were retested at room temperature it was observed that the diode forward voltages and reverse breakdown voltages were unaffected by the single temperature cycle; however, the on-resistances of each of the silicon diodes increased by approximately 14% after the single temperature cycle, and the on-resistance of the SiC diode increased by approximately 15% after the single temperature cycle. It is unknown at this point if this increase in on-resistance is a result of the temperature cycle on the packaging or the device itself, and it should be further investigated.

Based on the results, it can be concluded that silicon diodes are a good choice for cryogenic applications. The SiC diode, however, performed relatively poorly, primarily due to carrier freeze-out occurring at the low temperatures, and is not recommended for cryogenic applications.

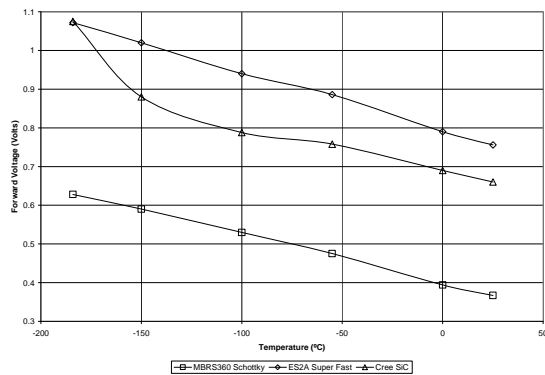


Fig. 10. Diode forward voltage vs. temperature.

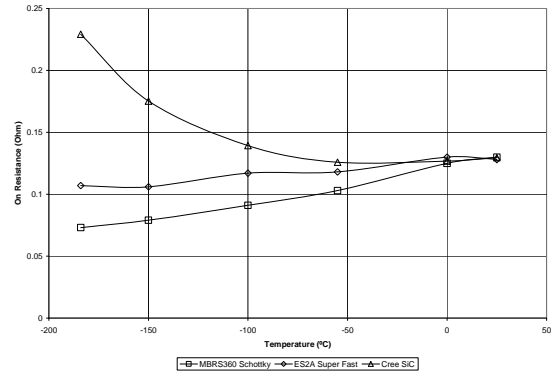


Fig. 11. Diode on-resistance vs. temperature.

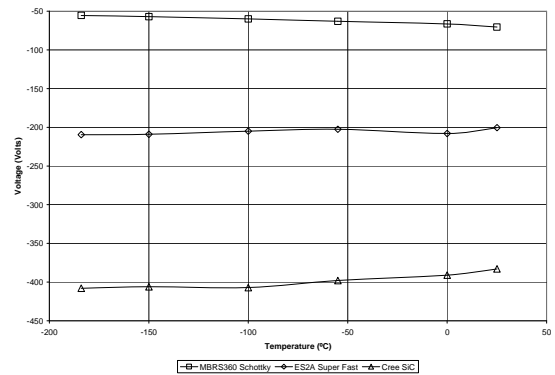


Fig. 12. Diode reverse breakdown voltage vs. temperature.

For the transistors, the following device technologies were examined: silicon MOSFET, SOI MOSFET, and SiC JFET. For each of the transistor technologies studied, the threshold voltages, on-resistances, and breakdown voltages were measured. BJT types of power devices were not investigated due to recent research efforts indicating poor performance of bipolar based parts when subjected to cold temperatures [1-3]. The following transistors were chosen to be tested: a 1.5 Amp 100 Volt silicon IRL110 HEXFET power MOSFET from International Rectifier, a 1.5 Amp 55 Volt SOI HTNFET from Honeywell, and a 5 Amp 1500 Volt SiC cascode JFET from SiCED. The cascode “device” consists of a silicon MOSFET in a cascode configuration with a normally-on SiC JFET. In addition to the cascode configuration of this device, cryogenic testing was performed on the MOSFET and JFET, each individually isolated. A Tektronix 371B programmable high power curve tracer was utilized to measure the threshold voltages, breakdown voltages, and on-state resistances of the transistors.

The threshold voltages for the silicon IRL110, the SOI HTNFET, and the SiCED cascode are shown in Fig. 13. The threshold voltage curve for the SiCED cascode is identical to the threshold voltage curve for the

MOSFET itself inside the SiCED cascode. From the figure it can be observed that as the temperature of these devices was decreased the threshold voltage increased. Fig. 14 shows the threshold voltage versus temperature for the normally-on SiC JFET itself within the SiCED cascode. It was observed that the threshold voltage for the SiC JFET decreased dramatically as the temperature was lowered. At room temperature (25 °C), the threshold voltage for the JFET was approximately -25 Volts. At -184 °C, the threshold voltage had decreased to approximately -51 Volts.

Fig. 15 and Fig. 16 show the on-resistance and breakdown voltage, respectively, for each transistor as the temperature was decreased. The results generally indicated a decrease in on-resistance for the silicon and SOI transistors as the temperature was lowered. The silicon MOSFET inside the SiC cascode exhibited a slight increase in on-resistance as the temperature was decreased. However, both the isolated SiC JFET and the SiC cascode circuit as a whole exhibited a slight decrease and then a dramatic increase in on-resistance as the temperature was lowered, much like the SiC schottky diode from Cree. It was observed that the primary change in on-resistance of the SiC cascode circuit was primarily dependent on the change in the on-resistance of the SiC JFET itself and not the MOSFET.

In the case of the breakdown voltages of the devices, the silicon and SOI transistor breakdown voltages both decreased slightly as the temperature was lowered. The breakdown voltage of the cascode MOSFET increased slightly, whereas the SiC JFET itself exhibited a relatively large change in breakdown voltage as the temperature was decreased. Fig. 16 shows that the breakdown voltage of the SiC cascode, was dominated largely by the change in the breakdown voltage of the JFET.

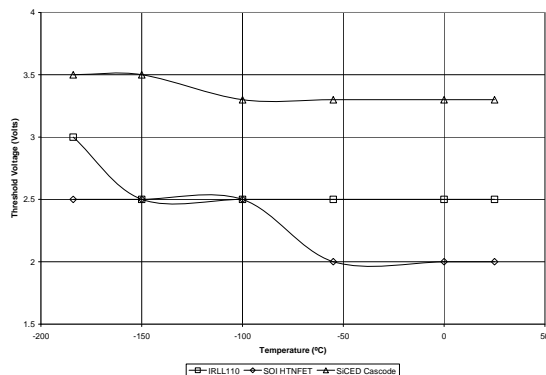


Fig. 13. Transistor threshold voltages for IRL1110, SOI HTNFET, and SiCED Cascode vs. temperature.

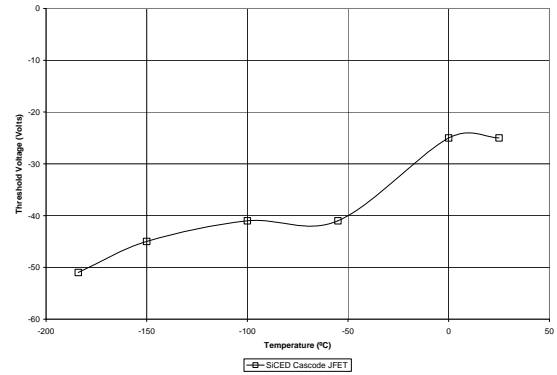


Fig. 14. Transistor threshold voltage for SiC JFET from SiCED Cascode vs. temperature.

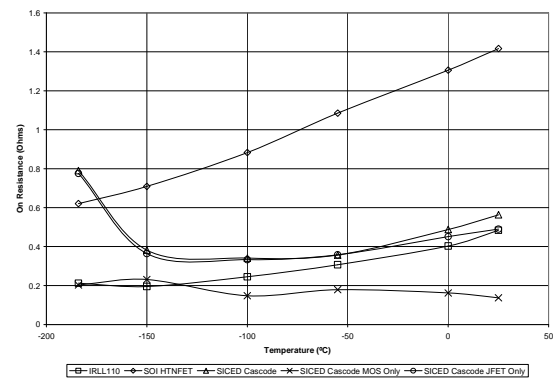


Fig. 15. Transistor on-resistance vs. temperature.

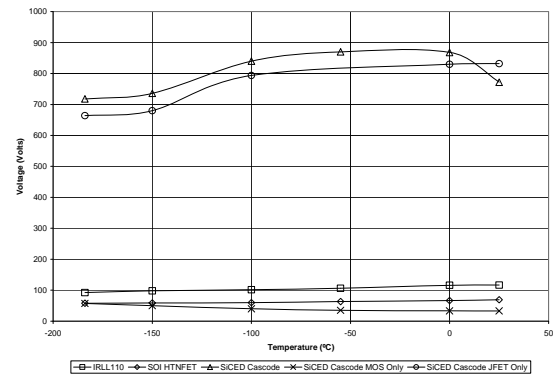


Fig. 16. Transistor breakdown voltage vs. temperature.

When the devices were retested at room temperature it was observed that the device characteristics were unaffected by the single temperature cycle.

Based on the results, it can be concluded that the silicon IRL1110 transistor would be the best choice for cryogenic applications, followed by the SOI transistor. The SiC transistor, however, performed relatively poorly, primarily due to carrier freeze-out occurring at

the low temperatures, and is not recommended for cryogenic applications.

5. DC MOTOR DRIVE POWER STAGE

A full bridge power stage was selected and designed to drive a 20 W Maxon RE 25 permanent magnet DC motor. The DC bus voltage was originally chosen to be 28 Volts in accordance with some of the DC bus voltages utilized in NASA rovers and probes; however, this was lowered to 24 VDC in order to not exceed the maximum continuous terminal voltage of the motor (i.e., 24 VDC).

The components for the power stage were chosen based upon the results of the cryogenic testing of the components. Because the power stage is a low voltage, low power design, the silicon IRL110 transistors (MOSFETs) were chosen as the power switches for the full bridge. The gate resistors were chosen to be the thick film type manufactured by Rohm. Polyethylene capacitors were chosen to serve the purpose of the DC bus filter capacitors. The power stage was constructed on an in-house made FR4 substrate and the components were mounted to it using standard Pb/Sn solder. The cryogenic power stage is shown in Fig. 17.

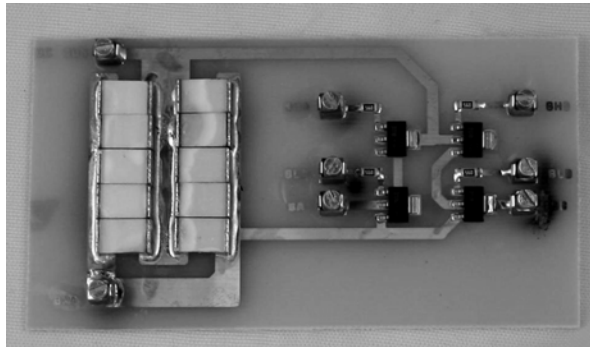


Fig. 17. Cryogenic power stage.

In order to test the power stage, the proper gate signals are needed to control the full bridge switches. These signals are generated from a control board which uses a L9903 motor bridge controller from ST Microelectronics. Since the controller has the capability to properly drive the gates of the IRL110 power switches, separate gate drivers were not necessary. This controller was kept outside the environmental test chamber during cold temperature testing since the power stage itself was being tested.

The Maxon RE 25 DC motor was kept outside the cryogenic tester. A smoothing inductor was connected in series with the motor (to decrease the current ripple) and both were connected to the motor connection wires of the power stage. As previously mentioned, the controller board was placed outside the test chamber

and it was connected to the power stage gate connection wires coming from the power stage inside the test chamber. Power was supplied to the controller board and the power stage using DC supplies and a PWM signal was supplied to the controller board using a function generator. Tektronix 3014B oscilloscopes were used to capture the waveforms of interest.

At each temperature test point, the power stage was energized and pressure was applied to the motor shaft in order to increase the output current delivered to the motor by the power stage to approximately 1 A average, which was followed by oscilloscope waveform captures. When the measurements at each temperature were compared with the room temperature measurements, the results indicated that there were no major changes to the power stage when operating at each temperature point.

After the final cold temperature measurement (at -184°C), the power stage was allowed to soak at this temperature (-184°C) for an additional 65 minutes with no power or signals applied to it. Following this long soak time, the power stage was again energized, pressure was applied to the shaft, and oscilloscope waveforms were captured. This longer soak time was implemented to see if being turned off while at an extreme low temperature for a longer period of time had any effect on the power stage operation. The results indicated that there were no detrimental effects caused by this additional soak time.

Following the additional soak time, the power stage was allowed to warm to room temperature and was again tested. This was done to determine what effects the complete temperature cycle might have had on the power stage. It was observed that there were no major changes to the power stage when subjected to one cold temperature cycle.

Fig. 18 shows the drain-to-source voltages of the power stage transistors when operating at room temperature (25°C). Fig. 19 shows the input and output voltages and currents of the power stage also operating at room temperature (25°C). In this waveform capture, channel 1 is the power stage input voltage, channel 2 is the power stage input current, channel 3 is the power stage output voltage, and channel 4 is the power stage output current.

Fig. 20 shows the drain-to-source voltages of the power stage transistors when operating at -184°C after the long soak time. Fig. 21 shows the input and output voltages and currents of the power stage when operating at -184°C after the long soak time. In this waveform capture the oscilloscope channel arrangements are identical to those as given in Fig. 19.

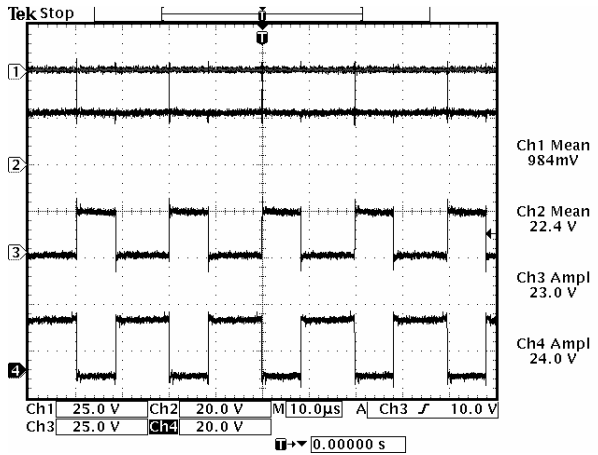


Fig. 18. Power stage drain-to-source voltages at 25 °C.

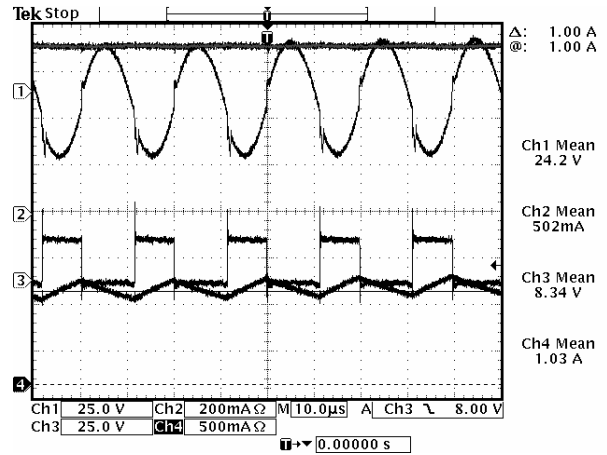


Fig. 21. Input voltage, input current, output voltage, and output current of power stage at -184 °C.

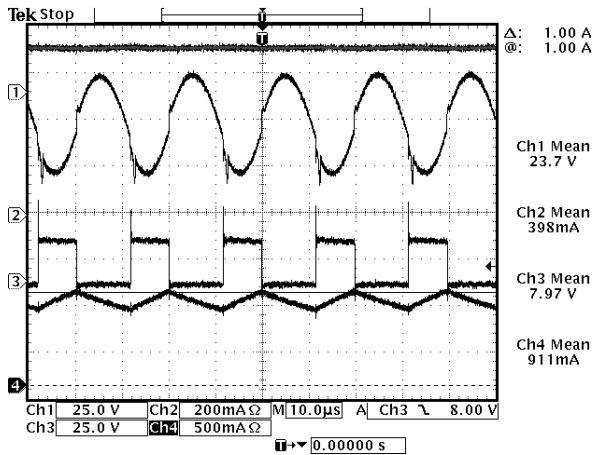


Fig. 19. Input voltage, input current, output voltage, and output current of power stage at 25 °C.

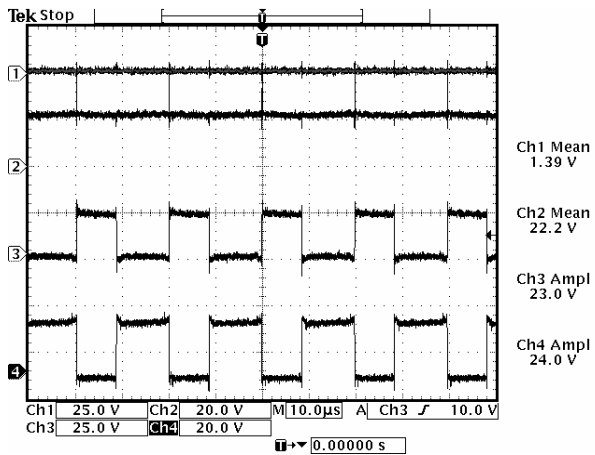


Fig. 20. Power stage drain-to-source voltages at -184 °C

6. SUMMARY

In this research the performance of commercially available passive and active components of varying technologies were cryogenically tested (down to -184 °C), including; resistors, capacitors, high/low side gate drivers, diodes, and transistors. Based upon the results of the cold temperature component testing, a 20 W DC motor drive full bridge power stage was constructed. The power stage was then successfully tested down to -184 °C while driving a permanent magnet DC motor.

7. REFERENCES

1. Elbuluk M., et al. "Power electronic components, circuits and systems for deep space missions", *IEEE Conference on Power Electronics Specialists*, Recife, Brazil, 2005, 1156 - 1162.
2. Elbuluk M., et al. "Performance of high-speed PWM control chips at cryogenic temperatures", *IEEE Transactions on Industry Applications*, Vol. 39, 443 - 450, 2003.
3. Elbuluk M., Hammoud A., "Power electronics in harsh environments", *IEEE Industry Applications Conference, 2005, Fortieth IAS Annual Meeting, Conference Record of the*, Hong Kong, China, 2005, 1442 - 1448.
4. Patterson R., et al. "Evaluation of capacitors at cryogenic temperatures for space applications", *Electrical Insulation, Conference Record of the 1998 IEEE International*, Washington, DC, United States, 1998, 468 - 471.
5. Hammoud A., Overton E., "Low temperature characterization of ceramic and film power capacitors", *Electrical Insulation and Dielectric Phenomena, 1996. IEEE 1996 Annual Report of the Conference on*, Millbrae, CA, United States, 1996, 701 - 704.